Performance Study of RPC Prototypes for the BESIII Muon Detector[*]

XIE Yu-Guang[1,2;1)]   ZHANG Jia-Wen[1]   LIU Qian[1,2]   HAN Ji-Feng[1,2]   QIAN Sen[1,2]

YAO Ning[1,3]   ZHAO Jian-Bing[1]   CHEN Jin[1]   LI Jian-Cheng[1]

1 (Institute of High Energy Physics, CAS, Beijing 100049, China)
2 (Graduate University of Chinese Academy of Sciences, Beijing 100049, China)
3 (Zhengzhou University, Zhengzhou 450052, China)

Abstract   In this paper, we describe a series of performance tests for the RPC prototypes of the BESIII muon detector. A new type of bakelite plate is made and the resistivity of samples is measured at different temperatures. Eight RPC prototypes are built and their performance as a function of the bakelite resistivity is studied. The rate capability of these chambers in the streamer mode is also studied by using a ^{137}Cs γ source. The results show that RPCs made of the new type of bakelite fulfill the requirements of the BESIII muon detector.

Key words   BESIII muon detector, RPC, bakelite resistivity, streamer mode

1   Introduction

The BESIII muon system has chosen Resistive Plate Chambers (RPCs)[1, 2] as its active detector for obvious reasons: low cost, good performance and suitable for industrial mass production. However, the experiences reported by some running RPC systems such as BaBar and Belle in recent years[3—5], especially the serious efficiency degradation in the oiled bakelite RPCs of BaBar muon chambers, have stimulated our R&D for developing a RPC using different materials. A new type of bakelite plate has been developed without linseed oiled coating, and the performance of the RPC using such materials is similar to or even better than those made of oiled bakelite or glass, as reported in Ref. [6]. In this paper, we report a detailed study of their performance as a function of bakelite properties.

2   Bakelite resistivity measurement

The resistivity is an important parameter of the bakelite plate with a major impact on the RPC performance. Six bakelite templates were made with a cross section of 12cm×12cm and their resistivity was measured in a temperature range from 16℃ to 29℃.
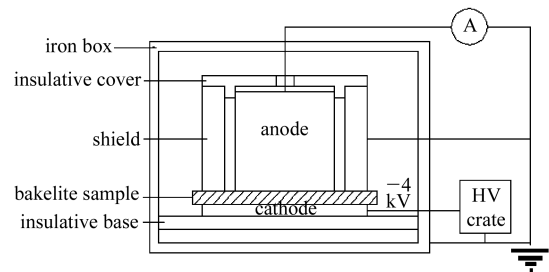

Fig. 1.   A schematic view of the resistivity measurement device.

The measurement device is shown in Fig. 1. The humidity was maintained by placing the measurement

device inside a sealed iron box. The resistivity of insulative materials as a function of the temperature can be given by the following empirical formula:

$$\rho_t = \rho_0 \cdot e^{Kt} \ , \tag{1}$$

i.e.

$$\ln \rho_t = \ln \rho_0 + Kt \ , \tag{2}$$

where, ρ_t is the resistivity at t℃, ρ_0 is the resistivity at 0℃, K is the slope. Fig. 2(a) shows the measurement results of all the six bakelite templates with a fit to Eq. (2). The fit result of K and $\ln \rho_0$ can be expressed as

$$K = \alpha + \beta \cdot \ln \rho_0 \ , \tag{3}$$

where, α and β are constants. Fig. 2(b) shows the fit results with

$$\alpha = 0.33 \pm 0.21, \quad \beta = -0.0164 \pm 0.0064.$$

In addiction, from Eq. (2) and Eq. (3), we also have:

$$K = \frac{\alpha + \beta \ln \rho_t}{1 + \beta t} \ , \tag{4}$$

hence,

$$\rho_{20} = \rho_t \cdot e^{K(20-t)} = \rho_t \cdot e^{\left[\frac{\alpha + \beta \ln \rho_t}{1 + \beta t}\right](20-t)} \ , \tag{5}$$

where, $0 \leqslant t < -1/\beta$. From Eq. (5) the bakelite resistivity at 20℃ can be derived from data at various temperatures.
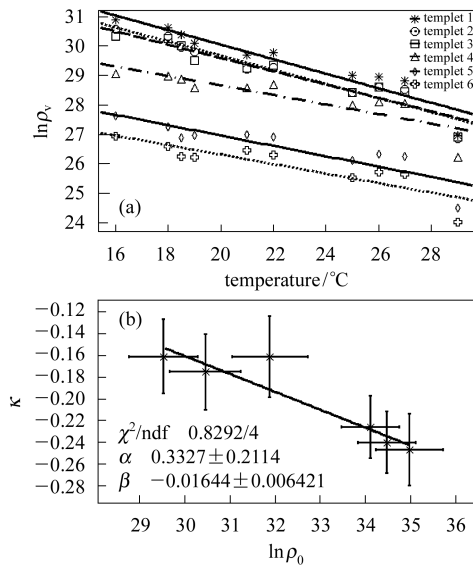

Fig. 2. (a) $\ln \rho_v$ of the bakelite template as a function of temperature. The lines are the fitting curves with Eq. (2); (b) Fitted parameters K and $\ln \rho_0$ showing a linear inverse relation.

3 Resistivity influence

3.1 Test setup

To judge the performance of a RPC running in the streamer mode, there are three most important indices: detection efficiency, single counting rate and dark current. The test results shown below are averaged over twelve continuous test runs. The test station is a traditional scintillator "telescope" system, as described in Ref. [6]. Eight chambers were trained more than three months before the test. Their averaged resistivity was listed in Table 1.

Table 1. Four groups of chambers with different resistivity.

group	No.	$\rho_v/(\Omega \cdot cm)$
A	1	2.45×10^{10}
	2	7.33×10^{10}
B	3	2.41×10^{11}
	4	4.12×10^{11}
C	5	3.91×10^{12}
	6	9.58×10^{12}
D	7	1.13×10^{13}
	8	1.36×10^{13}

Note: All data normalized to 20℃

All chambers are of the same dimension: 100cm×25cm. The relative permittivity of bakelite plates is from 2 to 6, the thickness of the graphite coating is 35±5μm and its surface resistivity is from 0.2MΩ/□ to 0.6MΩ/□. The thickness of the gas gap and the bakelite plates are all 2mm. Eight chambers were aerated in series and the gas mixture used is Argon/F134a/Isobutane (50/42/8). The test setup is shown in Fig. 3.
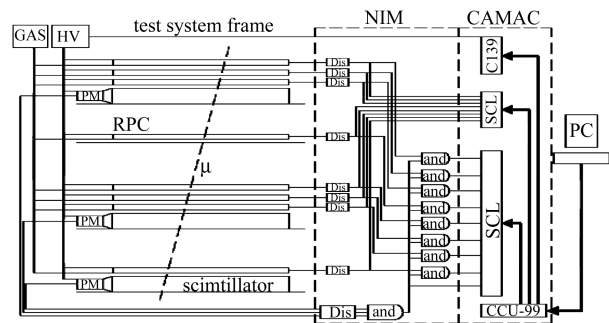

Fig. 3. Setup for RPC performance test. The "telescope" consists of three scintillators, and eight RPC prototypes are stacked in a column.

The induced signal is collected by readout strips, with each strip terminated by an 100Ω resistor to match its intrinsic impedance. The threshold of discriminators was set at 100mV. A DAQ program based on the Linux OS and ROOT framework was developed. The temperature and relative humidity, recorded by a slow control system[7], vary in $27\pm1.5°C$ and $45\pm15\%$ respectively.

3.2 Detection efficiency

A cosmic-muon is triggered by a three-fold coincidence of scintillators and the ratio of RPC fired events over that of the total cosmic-muon trigger gives the efficiency, which can be parameterized as

$$eff(x) = a_0 + \frac{eff_{\mathrm{plateau}}}{1 + e^{K(x - HV_{50\%})}} , \qquad (6)$$

where eff_{plateau} is the efficiency at the plateau, x is the high voltage, $HV_{50\%}$ is the high voltage at 50% efficiency, a_0 and K are fitting parameters.

The measured average efficiency as a function of applied high voltage is shown in Fig. 4, from which we can see the resistivity effects on the efficiency. They are distinguishable and dispersive. Although the efficiency slopes differ from each other and $HV_{50\%}$ spreads from 6.5kV to 7.2kV, all the efficiency shoulders are below 8kV, which is the planned operating high voltage of the BESIII muon detector. At 8kV, the plateau efficiencies of all chambers are higher than 95%.
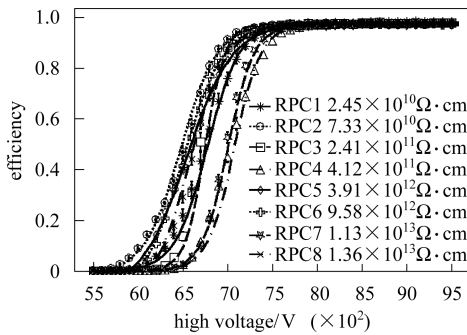

Fig. 4. The average efficiency of eight RPC prototypes as a function of high voltage. The lines are the fitting curves with Eq. (6).

3.3 Single counting rate

The single counting rate is the number of induced signals exceeding threshold per second per square centimeter, which is mainly due to the noise, closely re-

lated to the surface smoothness of the bakelite. Typically it follows a linear relation with the applied high voltage and can be parameterized as

$$R(x) = K_{\mathrm{rate}}(x - HV_{\mathrm{thrs}}), \quad x \geqslant HV_{\mathrm{thrs}} , \qquad (7)$$

where x is the high voltage, HV_{thrs} is the high voltage threshold for streamer to take place, K_{rate} is a fitting parameter.

As shown in Fig. 5, the single counting rate increases rapidly as the chamber resistivity decreases, and grows approximative linearly with the high voltage($<$12kV). For high resistivity chambers($\geqslant 2\times10^{11}\Omega\cdot$cm), the single counting rate rises much slower. At 8kV, the single counting rate of all high resistivity chambers is lower than 0.4Hz$\cdot$cm^{-2}.
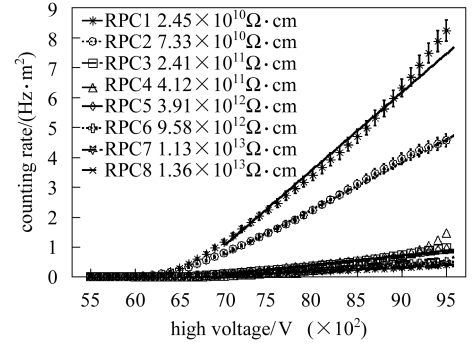

Fig. 5. The average single counting rate as a function of high voltage. The lines are the fitting curves with Eq. (7).

3.4 Dark current

The dark current originates primarily from the DC leakage current and the streamer charge in the gas gap. Similar to the result of single counting rate, dark current also shows a reverse relation with resistivity. The dark current can be parameterized as

$$I_{\mathrm{dark}}(x) = a_0 e^{K_{\mathrm{dark}}(x - HV_{\mathrm{thrs}})}, \quad x \geqslant HV_{\mathrm{thrs}} , \qquad (8)$$

where x is the high voltage, HV_{thrs} is the high voltage threshold for streamer to take place, K_{dark} and a_0 are the fitting parameters.

We can see in Fig. 6 that the dark current increases exponentially for low resistivity chambers, while linearly for the high resistivity chambers($\geqslant 4.12\times10^{11}\Omega\cdot$cm). At 8kV, the dark current of all high resistivity chambers is lower than 10μA$\cdot$m^{-2}.
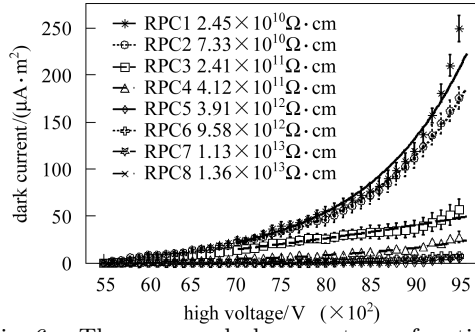
Fig. 6. The average dark current as a function of high voltage. The lines are the fitting curves with Eq. (8).

3.5 Resistivity control

The primary goal of this test is to find out a suitable resistivity range for the BESIII RPC mass production. As can be seen in Fig. 7, eff_{plateau} decreases linearly and K_{rate}, K_{dark} decrease exponentially as the logarithm of the resistivity. That means low resistivity is preferred for obtaining high eff_{plateau} and high resistivity is preferred for obtaining lower K_{rate} and K_{dark} coefficients. Hence, a compromise has been made to find an optimal resistivity range based on these three parameters. For the BESIII muon detector, the resistivity is chosen to be within $2.0 \times 10^{11} \Omega \cdot \text{cm}$ to $2.0 \times 10^{12} \Omega \cdot \text{cm}$ range, as
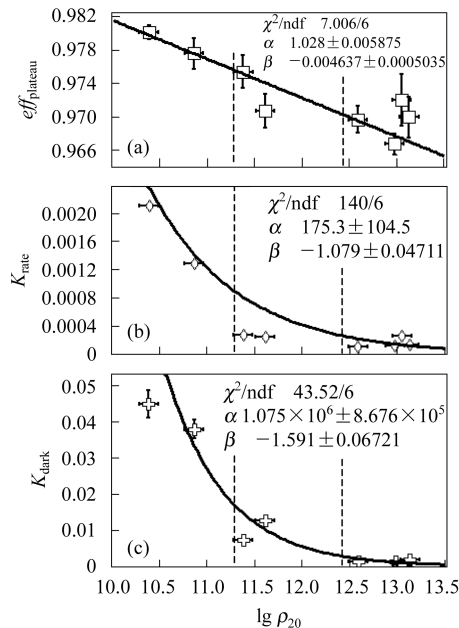

Fig. 7. The fitted parameters of eff_{plateau}, K_{rate} and K_{dark} as a function of logarithm of the chamber's resistivity at 20℃.
(a) eff_{plateau}, the solid line is a linear fit;
(b) K_{rate}; (c) K_{dark}; the solid curves are the exponential fitting curves.

indicated in Fig. 7.

4 Rate capability

4.1 Test setup

In order to simulate the actual operating environment and study the rate capability of our streamer mode RPCs, a 12mCi ^{137}Cs is chosen as the irradiation background[8] and three chambers selected from the above prototypes are tested in succession at the BEPC beam facility[9]. The test setup is illustrated in Fig. 8, with beams of e$^+$, e$^-$, p and π at the energy of 800MeV. The electrons and positrons can be identified online by a Cerenkov counter, and proton and pion can be identified offline by the Time-of-Flight spectrum, as described in Ref. [8]. The ^{137}Cs source was placed in front of RPC with an inclination angle of 45° with respect to the beam direction. The radiation intensity can be tuned by adjusting the central distance between ^{137}Cs and the RPC. One scintillator was located at the back of RPC, in coincidence with the beam trigger to measure the efficiency. The charge of signals is measured by an ADC through a linear Fan-in/Fan-out.
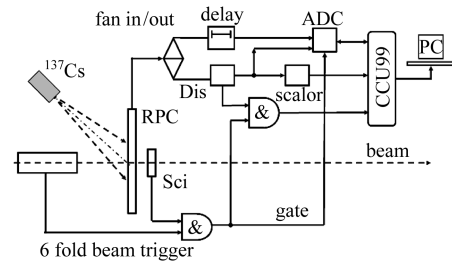

Fig. 8. The test setup for RPC rate capability.

4.2 Efficiency

Fig. 9 shows the efficiency of the tested chambers at a high voltage of 8kV as a function of the background γ radiation intensity in a beam of 800MeV for (a) mixed beam, (b) single pion, (c) single proton.

For low resistivity chambers, there is only 15% efficiency loss at 1000Hz·cm^{-2} and the efficiency is still more than 80%. But for high resistivity chambers, the efficiency loss is too large to be acceptable. On the other hand, the efficiency of single pions and single protons are less than that of the mixed beam due

probably to the positron backgrounds in the mixed beam, which tends to be absorbed rather than activating ionization. The BESIII muon detector requires the efficiency loss due to irradiation background be less than 10%. Therefore the background rate should be limited to less than 100Hz·cm^{-2} which is actually much higher than the case at BESIII running condition, as reported in Ref. [2].
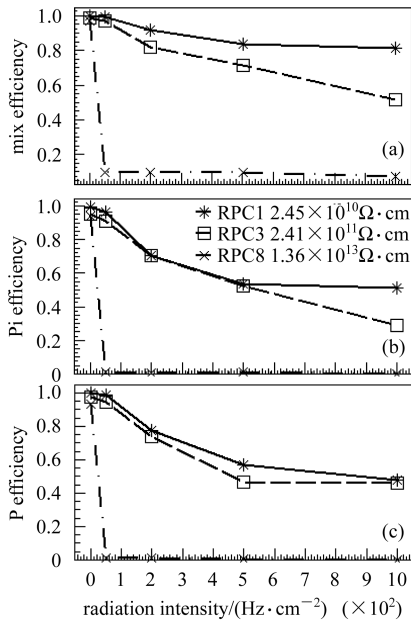

Fig. 9.　Efficiency loss of chambers with different resistivity affected by γ radiation.

4.3　Charge

How the irradiation influences the induced signal charge for a RPC is interesting since it may relate to the chamber efficiency and the aging effects.

The induced charge is read out by a 5cm×5cm copper pad and splitted by a Fan-in/Fan-out, and collected finally by a LeCroy 2249A ADC. The signal hence is attenuated by 5% and delayed by 100ns. The mean charge of RPC1 as a function of high voltage at different radiation intensities is shown in Fig. 10(a), which can be parameterized as

$$Q_{\mathrm{mean}}(x) = a\ln[K(x - HV_{\mathrm{thrs}})], \quad x \geqslant HV_{\mathrm{thrs}}, \quad (9)$$

where x is the high voltage, HV_{thrs} is the threshold high voltage for streamer operation, K and a are the fitting parameters.

The fitting parameter K, related to the induced charge suppression due to background radia-

tion intensity[10], is shown in Fig. 10(b). Its huge reduction may be one of the reasons that cause the efficiency degradation for a RPC in a strong γ radiation environment. However, after a total of 1.14×10^8 photons·cm^{-2} dose radiation for each chamber, no irretrievable damage or aging effect due to hard radiation is observed.
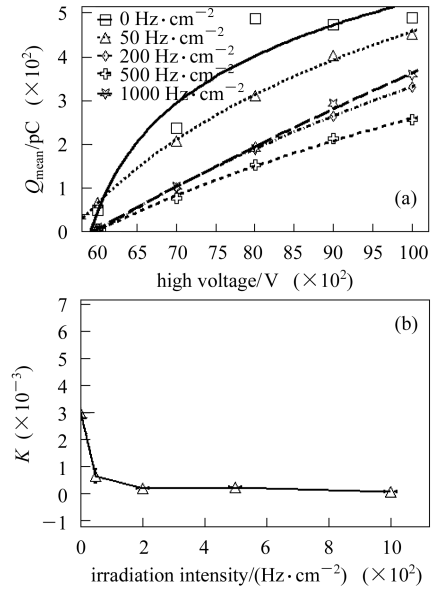

Fig. 10.　The mean charge of RPC1 as a function of high voltage at different radiation intensities. The lines in (a) are the fitting curves with Eq. (9); (b) Fitted parameter K vs. background irradiation intensity.

5　Conclusion

We made several RPCs with new surface treated bakelite and tested them in our lab as well as in a beam at BEPC. The test results of the bakelite resistivity as a function of temperature agree with the empirical formula. The plateau efficiency of RPC is inversely proportional to the chamber resistivity, while both single counting rate and dark current increase rapidly with the decrease of resistivity. For the chambers within the selected resistivity range from $2.0\times10^{11}\Omega\cdot$cm to $2.0\times10^{12}\Omega\cdot$cm, the efficiency is higher than 95%, single counting rate is less than 0.4Hz·cm^{-2}, and dark current is lower than 10μA·m^{-2} at 8kV. The beam test results show that low resistivity chambers have better rate capability. For a rate up to 100Hz·cm^{-2}, the efficiency loss of the chambers

is less than 10% at 8kV. All the test results described above show that the new type of bakelite RPC meets the requirement of the BESIII muon detector.

References

1 Santonico R, Cardarelli R. Nucl. Instrum. Methods, 1981, **187**: 377
2 BESIII Preliminary Design Report. IHEP BEPCII SB 13, 2004
3 Bruno G. Eur. Phys. J., 2004, **C33**: s01, s1032–s1034
4 Anulli F et al. Nucl. Instrum. Methods, 2003, **A515**: 322—327
5 Va'vra J. Nucl. Instrum. Methods, 2003, **A515**: 354—357
6 ZHANG Jia-Wen et al. Nucl. Instrum. Methods, 2005, **A540**: 102
7 XIE Xiao-Xi et al. Nuclear Electronics & Detection Technology, 2005, **29**(5): 475 (in Chinese)
(谢小希等. 核电子学与探测技术, 2005, **29**(5): 475)
8 Carboni G et al. Nucl. Instrum. Methods, 2004, **A533**: 107—111
9 LI Jia-Cai et al. HEP & NP, 2004, **28**(12): 1269—1277 (in Chinese)
(李家才等. 高能物理与核物理, 2004, **28**(12): 1269—1277)
10 Abbrescia M et al. Nucl. Instrum. Methods, 1997, **A392**: 155—160

BESⅢ μ探测器阻性板模型室的性能研究*

谢宇广[1,2;1)]　　张家文[1]　　刘倩[1,2]　　韩纪峰[1,2]　　钱森[1,2]　　姚宁[1,3]　　赵建兵[1]　　陈进[1]　　李建成[1]

1 (中国科学院高能物理研究所　北京　100049)
2 (中国科学院研究生院　北京　100049)
3 (郑州大学　郑州　450052)

摘要　对基于酚醛树脂的阻性板室(RPC)进行研究. 通过改进的表面处理工艺, 开发了一种新的阻性板材料, 并在不同温度下对多块样板的电阻率进行了测量. 对比了基于此新型阻性板的不同电阻率RPC模型室的探测效率、计数率和暗电流. 利用 ^{137}Cs γ 源和实验束流研究了流光模式RPC的抗辐照性能. 结果表明此新型阻性板RPC满足BESⅢμ探测器的要求.

关键词　BESⅢμ探测器　阻性板室　酚醛树脂电阻率　流光模式